# Mechanical Properties and Failure Mode of Thermoplastic Elastomers from Natural Rubber/Poly(methyl methacrylate)/Natural Rubber-*g*-Poly(methyl methacrylate) Blends

ZACHARIAH OOMMEN, SABU THOMAS

School of Chemical Sciences, Mahatma Gandhi University, Priyadarshini Hills P.O., Kottayam-686 560, Kerala, India

**ABSTRACT:** The mechanical properties and fracture behavior of natural rubber/poly-(methyl methacrylate) blends were investigated as a function of composition, graft copolymer concentration, and mixing conditions. The mechanical properties and failure behavior vary with the blend ratio, graft copolymer concentration, and mixing conditions. Various two-phase models were used to fit the experimental mechanical properties. Mechanical properties such as stress–strain behavior, tensile strength, tensile modulus, tear strength, and Izod impact strength were evaluated as a function of compatibilizer concentration. The domain size of the dispersed phase decreases with graft copolymer concentration followed by a leveling off at higher concentration. The mechanical properties attain a maximum value at the leveling point, which is an indication of interfacial saturation and the attainment of maximum interfacial adhesion between the homopolymers. Tensile and tear fracture surfaces were examined by scanning electron microscopy. The detachment of the dispersed domains from the matrix is an indication of no adhesion between the two phases in the case of uncompatibilized blends. Microfibrils between the matrix and the dispersed phase indicate a sign of interfacial adhesion between the phases in the case of compatibilized blends. © 1997 John Wiley & Sons, Inc. J Appl Polym Sci **65:** 1245–1255, 1997

## INTRODUCTION

Polymer blends are gaining more importance as they combine the characteristics of individual polymers. Although blending looks very attractive, most of the polymer blends are immiscible and incompatible. Reasons for incompatibility are high interfacial tension and poor interface adhesion. It is well known that the addition of a block or graft copolymer makes the immiscible polymer pairs more compatible.[1,2] According to Paul and Newman,[3,4] the addition of a copolymer reduces the interfacial tension, permits a finer dispersion, provides a measure of stability against gross segregation, and results in improved interfacial adhesion.

Thermoplastic elastomers (TPEs) are a relatively new class of materials which combine the physical properties of elastomers and the excellent processing characteristic of thermoplastics.[5–8] The thermoplastic elastomers are usually prepared either by melt-mixing or solution-mixing techniques. The mechanical properties of the resulting TPEs are poor due to the incompatibility between the individual components. Several studies have been reported on the properties and application of various TPEs.[9–11] Properties of ethyl-

ene propylene diene monomer/polypropylene (EPDM/PP) thermoplastic blends, by partial crosslinking of the elastomer phase, were reported by Fisher.[12] Campbell et al.[13] described the method of preparation, injection-molding conditions, and physical properties of natural rubber/polyethylene (NR/PE) and NR/polypropylene (PP) blends. Coran and Patel[14–16] published a series of articles on rubber–thermoplastic blends and attempted to correlate their physical properties with the fundamental characteristics of the elastomer and thermoplastic components. Rheology, morphology, and mechanical properties of various thermoplastic elastomeric blends were reported by Thomas and coworkers.[17,18]

Recently Thomas and coworkers[19,20] reported on the mechanical properties of TPEs from acrylonitrile butadiene rubber/PP (NBR/PP) and acrylonitrile butadiene rubber/high-density polyethylene (NBR/HDPE) prepared by reactive compatibilization. The improvement in tensile impact strength was explained on the basis of size, shape, and distribution of the rubber phase in the plastic matrix. The increase in mechanical properties with increase of compatibilizer concentration was correlated to the reduction in particle size of the dispersed NBR phase. Recently, Asaletha et al.[21] studied the effect of the addition of a graft copolymer on the mechanical properties of the NR/polystyrene blend and attempts have been made to correlate the mechanical properties with the morphology of the system.

TPEs are generally used for making automobile parts where processes such as abrasion, flexing, and tear are prominent factors leading to the fracture of the products. Since these materials find uses in a variety of applications, a thorough understanding of their failure mode is important in predicting their service life. Scanning electron microscopy (SEM) has been successfully used to study the failure properties of rubbers and rubber-based compositions.[22–24]

TPEs from NR and poly(methyl methacrylate) (PMMA) were recently prepared by Oommen and Thomas.[25,26] A graft copolymer of NR and PMMA was used for compatibilizing the system. Morphology and melt flow behavior of the blends were analyzed in detail. In this article, we report the results of our studies on the mechanical properties (tensile, tear, and Izod impact behavior) of TPEs prepared by blending NR and PMMA. The influence of composition, graft copolymer concentration, and mixing conditions on the mechanical

properties are discussed in detail. Various two-phase models were used to predict the mechanical properties of these blends. Failure topography of the samples was examined using scanning electron microscopy.

## EXPERIMENTAL

### Materials

The poly(methyl methacrylate) (PMMA) used in this study was supplied by Gujarat State Fertilizer Corp. Natural rubber (ISNR 5 Indian standard natural rubber, NR) was supplied by the Rubber Research Institute of India, Kottayam. Graft copolymer NR-g-PMMA was prepared in our laboratory by polymerizing methyl methacrylate (MMA) in the presence of rubber latex using a redox initiator consisting of cumene hydroperoxide and tetraethylenepentammine. NR latex particles are swollen with MMA, which is then polymerized at room temperature for about 24 h. The graft is purified by the fractional precipitation method. Free PMMA and NR are removed using acetone and petroleum ether, respectively. The purified graft copolymer is dried in a vacuum oven. The amounts of grafting efficiency and PMMA grafted were 60 and 25%, respectively. These values were obtained gravimetrically as reported earlier.[25,26] Grafting was confirmed by the separation of a high molecular weight component from the GPC eluate. The IR and H-NMR spectroscopic studies further confirmed the formation of the graft copolymer. The IR spectrum of the graft copolymer shows intense absorption at 1730 and 1140 cm$^{-1}$, corresponding to the $\diagdown C = O$ and (C—O) group in the methacrylate chain along with the characteristic absorption of the NR group. The H-NMR spectrum obtained at 90 MHz shows chemical shifts at 1–2, 3–4, and 4.6–4.8 $\delta$, corresponding to alkyl, OCH$_3$, and vinyl protons, respectively. H-NMR analysis indicated that the percent of MMA grafted onto the NR backbone is 26%, which is in agreement with the gravimetric determination. Dynamic mechanical spectroscopy studies of the graft copolymer showed two transitions corresponding to NR ($-50°C$) and PMMA ($135°C$). This suggests that the copolymer is sufficiently phase-separated and can be located at the interface. The molecular weight determina-

**Table I   Characteristics of the Materials**

| Materials | Density $(g/cm^3)$ | Solubility Parameter $(cal/cm^3)^{1/2}$ | Intrinsic Viscosity $(dL/g)$ (Toluene) | Molecular Weight $(\bar{M}_w)$ |
|---|---|---|---|---|
| NR | 0.90 | 7.75 | 4.35 | $8.05 \times 10^5$ |
| PMMA | 1.18 | 11.80 | 0.42 | $2.09 \times 10^5$ |
| NR-$g$-PMMA | 1.04 | — | 3.20 | $8.76 \times 10^5$ |

tion of NR, PMMA, and NR-$g$-PMMA by the viscometry method (Table I) supports the above observations.

### Blend Preparation

NR and PMMA were blended together in toluene (5%) in different proportions. The blends were referred to as $N_0$, $N_{30}$, $N_{50}$, $N_{70}$, and $N_{100}$, where the subscripts denote the wt % of the NR. Solution-cast blends of $N_{50}$ were also made with and without the addition of the graft copolymer (NR-$g$-PMMA). After mixing NR, PMMA, and the graft copolymer in toluene, the mixture was kept overnight and then stirred for 10 h using a magnetic stirrer at ambient temperature. The blend films were cast onto a glass plate. The films were dried in a vacuum oven at 90°C until the last traces of solvents were removed. 50/50 NR/PMMA solution-cast blends with 0, 5, 10, and 15% graft copolymer are denoted by $0N_{50}$, $5N_{50}$, $10N_{50}$, and $15N_{50}$, respectively.

Samples were also prepared by melt mixing the components. Melt mixing was carried out using a Brabender Plasticorder PLE 651 at a temperature of 145°C and at a rotor speed of 80 rpm. PMMA was melted for 2 min and then blended with NR for another 2 min. Finally, the compatibilizer was added and blended for another 4 min. The molten mixture was removed from the Brabender mixing bowl, sheeted on a mill, and compression-molded into thin sheets of 2 mm thickness. The melt-mixed 50/50 NR/PMMA blend with 0, 5, 10, and 15% graft copolymer are denoted by $0N'_{50}$, $5N'_{50}$, $10N'_{50}$, and $15N'_{50}$, respectively.

### Determination of Tensile Strength, Tear Strength, and Izod Impact Strength

Tensile strength and elongation at break of the samples were measured at 25°C according to the ASTM D638 specification using dumbbell-shaped test pieces at a crosshead speed of 500 mm/min

using a Zwick universal testing machine. The tear strength of the sample was determined according to ASTM D624-81 using 90° angle test pieces. The temperature and crosshead speed used were the same as that for tensile strength measurements. The Izod impact strength of samples was measured according to the ASTM D256 test method. The dimensions of the specimen used were 6.13 × 1.20 × 1.23 cm. The impact energy was obtained by the difference of the potential energy of the falling hammer before and after impact. Impact energy per unit breadth of the sample is expressed as the impact strength. The machine used in the present investigation was a Ceast 6546/0000. The average values of at least five tests are reported in every case.

### Scanning Electron Microscopy (SEM) Studies

The SEM observations of the tensile and tear failure surface were made using a scanning electron microscope (JOEL 35 CF). The failure surface of the test samples were carefully cut and sputter-coated with gold and then examined under the microscope.

## RESULTS AND DISCUSSION

### Effect of Blend Ratio on Morphology and Mechanical Properties

#### Morphology of the Blend

The scanning electron micrographs of the blends $N_{70}$, $N_{50}$, and $N_{30}$ are given in Figure 1(a–c). In $N_{70}$, the PMMA phase is dispersed as domains in the continuous NR matrix. The average size of the dispersed domain is 8.9 $\mu$m. As the PMMA content increases from 30 to 50 wt %, the particle size increases to 18.3 from 8.9 $\mu$m. The size dimensions reported are averages of about 100 domains obtained from different photographs of the same sample. The increase in size is due to the agglom-
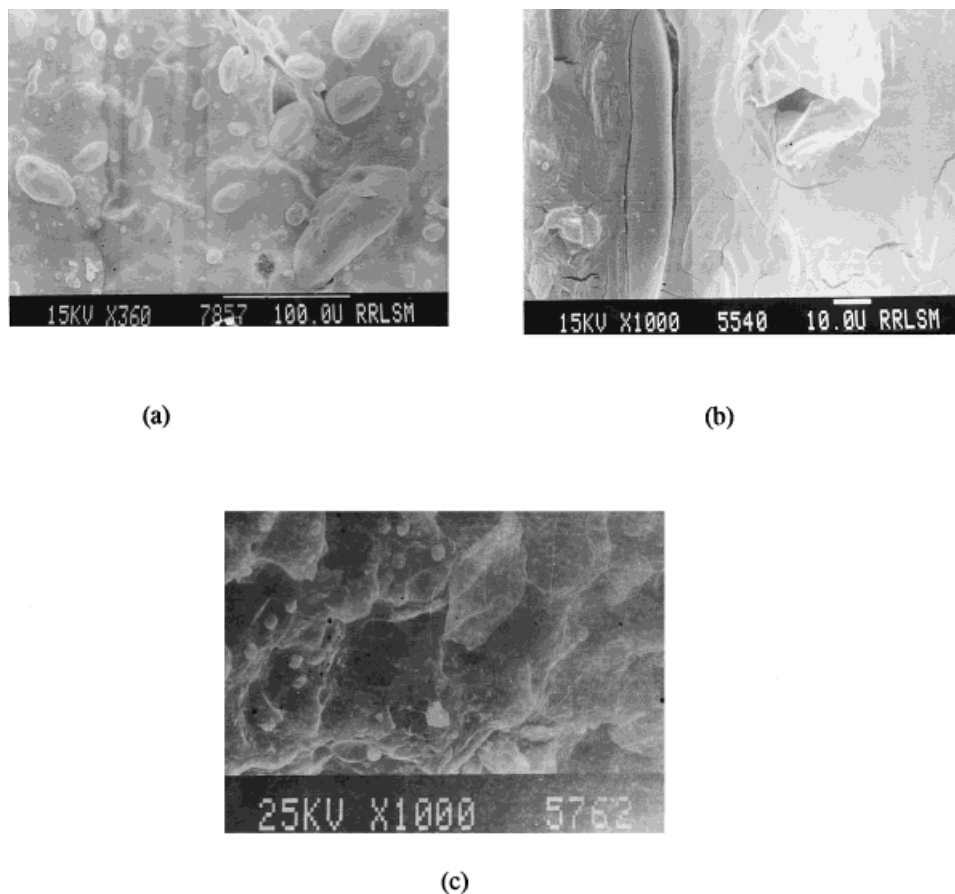
(a)



(b)



(c)

**Figure 1**    Scanning electron micrograph of NR/PMMA blends: (a) 70/30; (b) 50/50; (3) 30/70.

eration/coalescence of the dispersed particles. The occurrence of the coalescence at higher concentration of one of the components has been reported by many authors.[27-29] In the $N_{30}$ blend, both NR and PMMA phases exist as a co-continuous phase. The particle size and size distribution are given in Figure 2.

### Mechanical Properties

The mechanical properties of NR/PMMA blends as a function of the blend ratio is given in Table II. The stress–strain curves of $N_0$, $N_{30}$, $N_{50}$, $N_{70}$, and $N_{100}$ given in Figure 3 clearly show the deformation nature of the blends under an applied load. PMMA shows the brittle nature and high modulus. Addition of NR reduces the moduli of the blend as evidenced from the stress–strain curve. The blend becomes more ductile as the NR content increases. The improved rubbery behavior of $N_{70}$ compared to $N_{50}$ and $N_{30}$ can be explained

in terms of the phase inversion of PMMA from a dispersed to a continuous phase on passing from $N_{70}$ to $N_{30}$. Neat NR exhibits the behavior of a typical uncrosslinked elastomer. Elongation at break decreases and the Young's modulus increases as the percentage of NR decreases. Pure PMMA shows higher tensile strength, tear strength, and Young's modulus. These properties decreased as the NR content increased. The properties do not obey the additivity rule and exhibit negative deviation. The observed negative deviation is due to the poor interfacial adhesion between the polar PMMA and nonpolar NR phases which causes a poor stress transfer between the matrix and the dispersed phase. Again, the change in mechanical property is not completely linear with composition.

### Model Fitting

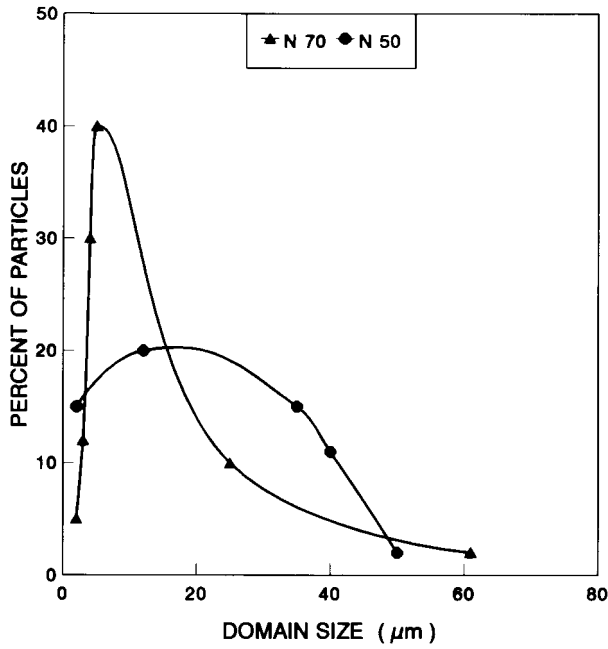Various composite models have been used to predict the mechanical properties of these blends.

**Figure 2**   Effect of blend composition on the domain size distribution of 70/30 and 50/50 NR/PMMA blends.



**Figure 3**   Stress–strain curves of NR/PMMA blends as a function of composition.

The highest upperbound parallel model is given by the rule of mixtures:

$$M = M_1\phi_1 + M_2\phi_2 \tag{1}$$

where $M$ is the mechanical property of the blend; $M_1$ and $M_2$, the mechanical properties of components 1 and 2, and $\phi_1$ and $\phi_2$, the volume fraction of the components 1 and 2, respectively. The low-
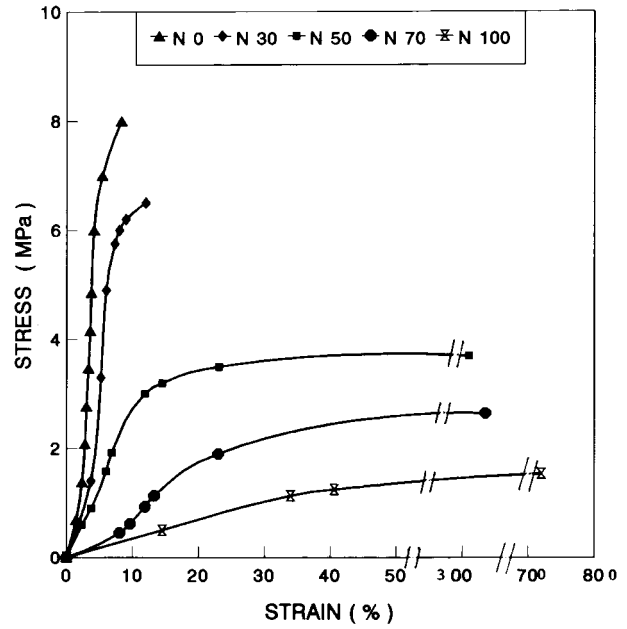
est lower-bound series model is given by the equation

$$\frac{1}{M} = \frac{\phi_1}{M_1} + \frac{\phi_2}{M_2} \tag{2}$$

where $M$, $M_1$, $M_2$, $\phi_1$, and $\phi_2$ have the same significance as in the parallel model. According to the Halpin–Tsai equation,

**Table II   Mechanical Properties of NR/PMMA Blends**

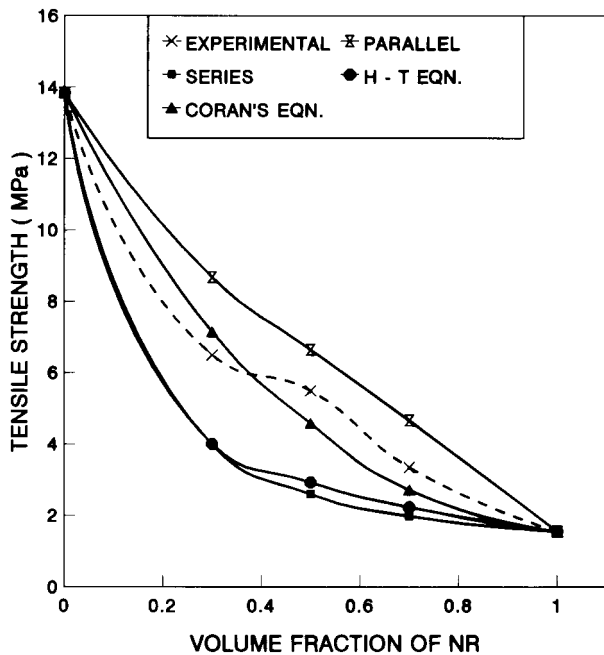| Blend Composition | Tear Strength (N/mm) | Elongation at Break (%) | Tensile Strength (N/mm²) | Young's Modulus (N/mm²) |
|---|---|---|---|---|
| $N_{100}$ | 3.62 (0.27) | 712 (51) | 1.54 (0.18) | 14.9 (1.41) |
| $N_{70}$ | 6.12 (0.52) | 365 (24) | 2.65 (0.32) | 10.2 (0.77) |
| $N_{50}$ | 9.5 (0.69) | 322 (10) | 3.75 (0.23) | 17.5 (1.08) |
| $N_{30}$ | 16.5 (0.77) | 12 (1.4) | 6.5 (0.58) | 167 (8.71) |
| $N_0$ | 33.5 (3.0) | 9 (0.63) | 8.0 (0.88) | 178 (5.17) |

Standard deviation values are given in parentheses.

**Figure 4** Experimental and theoretical values of tensile strength as a function of volume fraction of NR.

$$\frac{M_1}{M} = \frac{1 + A_i B_i \phi_2}{1 - B_i \phi_2} \qquad (3)$$

$$B_i = \frac{(M_1/M_2 - 1)}{(M_1/M_2 + A_i)} \qquad (4)$$

In the Halpin–Tsai equation,[30,31] subscripts 1 and 2 refer to the continuous phase and dispersed phase, respectively. The constant $A_i$ is defined by the morphology of the system. For the plastic domain dispersed in a continuous elastomeric matrix, $A_i = 1.5$. For an incompatible blend, the mechanical properties are generally between the parallel model upper bound and the series model lower bound.

According to Coran's equation,[32]

$$M = f(M_U - M_L) + M_L \qquad (5)$$

where $f$ can vary from 0 to unity. The value of $f$ is a function of phase morphology. The value of $f$ is given by

$$f = V_H^n(nV_S + 1) \qquad (6)$$

where $n$ is related to the phase morphology. $V_H$ and $V_S$ are the volume fractions of the hard and soft phases, respectively. The change in $f$ with respect to $V_H$ is greatest when $V_H = (n - 1)/n$; thus, the value of $(n - 1)/n$ could be considered as the volume fraction of the hard-phase material that corresponds to a phase inversion.

Figures 4 and 5 show the experimental and theoretical curves of tensile strength and tear strength, respectively, as a function of soft-phase volume fraction. It can be seen that experimental data are close to Coran's model in which $n = 1.5$. The value of $n = 1.5$ corresponds to a $V_H = 0.33$, where there is a phase inversion in the blend.

## Effect of Graft Copolymer on Mechanical Properties

### Tensile, Tear, and Izod Impact Properties

The stress–strain curve of 50/50 NR/PMMA as a function of compatibilizer loading is given in Figure 6. The deformation nature of the blend varies with the graft copolymer concentration. The pure blend shows a very low value of stress up to 300% elongation, where it breaks. The addition of the graft copolymer changes the deformation nature of the curve considerably. For the blends with 5, 10, and 15% graft, the stress increases almost linearly and failure occurs. The tensile strength of the 50/50 NR/PMMA blends
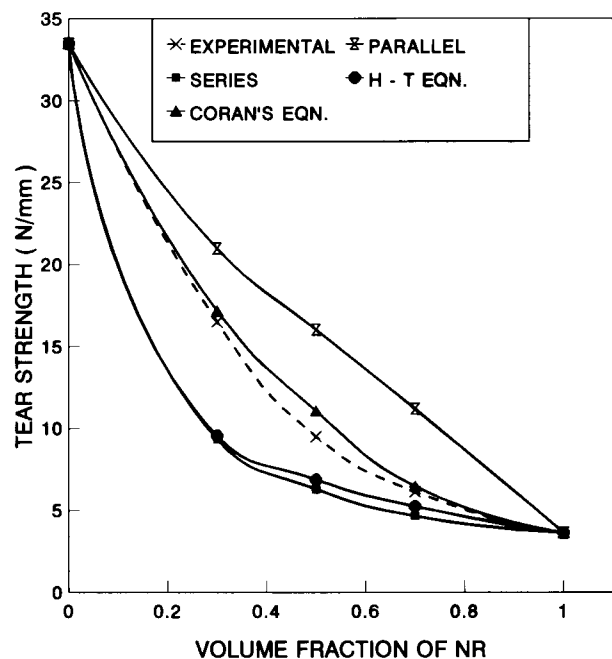


**Figure 5** Experimental and theoretical values of tear strength as a function of volume fraction of NR.
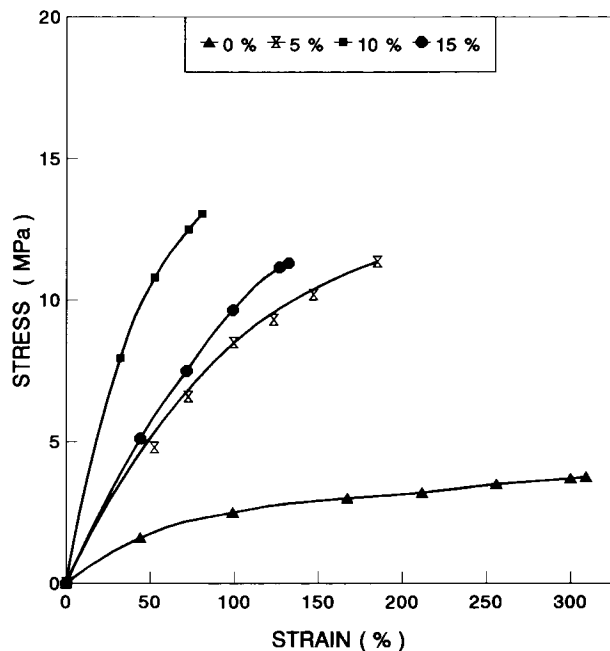
**Figure 6** Stress–strain curves of NR/PMMA blends as a function of graft copolymer concentration.

with the graft copolymer prepared by solution-cast techniques and melt-mixed methods are given in the Table III. The 50/50 NR/PMMA blend with no graft copolymer has a low tensile strength and exhibits considerable improvement by the addition of the graft copolymer. Tensile strength increases and reaches a leveling off at 10% graft copolymer concentration. Further addition makes only a little change in the tensile strength. Barentsen and Heikens[33] reported that addition of the graft copolymer improves the strength and modulus of PS–LDPE blends. However, the elongation at break decreases with graft copolymer concentration. The stress–strain behavior of the melt-mixed blend (Table III) also shows a similar trend as that of the solution-cast blends. Tear and Izod impact strength of the 50/50 NR/PMMA blend as a function of the graft copolymer concentration is also given in Table III. These properties follow a similar pattern as that shown in the case of tensile properties. The uncompatibilized blend exhibits low tear strength values.

The NR/PMMA blend remains incompatible in the pure state due to the dissimilar chemical nature and, therefore, the mechanical properties are poor. Addition of the graft copolymer improves the mechanical properties tremendously. The effect of

the graft copolymer is to increase the adhesion between the immiscible polymers and to provide a fine degree of dispersion. Thomas and Prud'homme[34] reported on the so-called interfacial saturation of binary polymer blends by the addition of a compatibilizer. The presence of the graft copolymer reduces the domain size considerably and the polydispersity is reduced.

The reduction in the size of the dispersed phase is in agreement with the variation of the tensile strength. The tensile strength of uncompatibilized 50/50 NR/PMMA blend is 3.7 N/mm$^2$ and the domains show an average size of 183 $\mu$m. The graft copolymer addition (5%) reduces the domain size tremendously and the tensile strength shows a 300% increase. The reduction in domain size and increase in tensile strength continue until the interface is saturated. The saturation of the interface is indicated by the leveling-off of the domain size and tensile properties (Table III).

The low tear strength of the uncompatibilized system indicates lack of adhesion between the two components. The change in tear and Izod impact strength of the blend with graft copolymer concentration can be explained in terms of the morphology of the system. Addition of the graft copolymer reduces the size of the dispersed PMMA domains. The distribution of particles also becomes uniform. The reduction in particle size is due to the reduction in interfacial tension and the increased interfacial adhesion. This will help to inhibit the propagation of a growing crack during tearing. Hence, compatibilization enhances the resistance to tear. As in the case of the tensile properties, the leveling-off observed in tear strength at 10% graft copolymer is also due to the interfacial saturation. Again, melt-mixed blends exhibit lower tear strength compared to solution-cast blends.

Impact resistance can be improved by the incorporation of small elastomeric particles into the matrix. Borggreve et al.[35] showed that both size and concentration of the rubber phase have considerable effects on the impact strength of nylon–rubber blends. A study by Wu[36] indicated that the particle size of rubber in nylon 6,6 increases from 0.8 to 1.73 $\mu$m as the rubber content increases from 10–25%. Borggreve et al.[37] further demonstrated that critical interparticle spacing is not uniform but increases with the test temperature from 0.1 $\mu$m at −35°C to 1 $\mu$m at 80°C. It is clear from the results that the interfacial adhesion is an important factor in rubber toughening. According to Shaw and Singh,[38] the observed in-

crease in the impact strength of PS/EPDM-*g*-styrene/EPDM is due to the improved interfacial adhesion. However, the reduction in impact strength for the blend containing 15% graft copolymer is due to the formation of compatibilizer micelles in the homopolymer phase. Similar results were recorded by Nando and coworkers.[39]

## Comparison of Mechanical Properties Between Melt-Mixed and Solution-Cast Blends

A comparison of tensile strength and tear strength of the solution-cast and melt-mixed samples was carried out. Even though both systems exhibit considerable improvement in mechanical strength, the melt-mixed samples were found to show lower strength values as compared to respective solution-cast samples (Table III). Melt-mixed blends exhibit lower strength both in the compatibilized and uncompatibilized states compared to the solution-cast system. The improved strength of the solution-cast blend is because molecular-level mixing is achieved during solution mixing and this leads to improved adhesion between the phases. The high shearing action (80 rpm) and temperature (145°C) employed during the preparation of the blend by the melt-mixing technique might have caused degradation of NR and PMMA, resulting in substantial reduction in strength. Molecular weight determination of NR after the melt-mixing process gave evidence of the degradation of NR. The molecular weight $\bar{M}_w$ of

the NR before melt mixing was $7.02 \times 10^5$. This value decreases to $3.49 \times 10^5$ after melt mixing.

### Failure Topography

Figure 7 shows the tensile fracture surface of 50/50 NR/PMMA blends with and without the graft copolymer. The fracture surface [Fig. 7(a)] of the uncompatibilized blend, $0N_{50}$, exhibits an elastic-type deformation with discontinuous fracture paths. The detachment of the dispersed phase shows no adhesion between the two phases. The PMMA domains have undergone deformation during tensile testing. This is evident from the elongated PMMA domains present in the fracture surface. In the compatibilized blends $5N_{50}$, $10N_{50}$, and $15N_{50}$ [Fig. 7(b–d), the dispersed domains are small in size and the area of contact is larger. The microfibrils between the matrix and the dispersed phase show signs of interfacial adhesion between the two phases. Similar findings were reported by Heikens and coworkers.[40] These observations indicate that the copolymer acts as an interfacial agent by reducing the average dimensions of the dispersed phase. The high tensile strength values of the compatibilized blends are in agreement with the above facts.

Tear fractographs are given in the Figure 8. Figure 8(a) gives the tear fracture surface of $0N_{50}$. The PMMA domains are large, irregular, and nonspherical. Voids are created by the detachment of domains of the dispersed phase. This

**Table III    Mechanical Properties of 50/50 NR/PMMA Blends with Graft Copolymer**

| Graft Copolymer (%) | Solution-Cast System | | | | Melt-Mixed System | | | |
| | Average Domain Size (μm) | Tear Strength (N/mm) | Elongation at Break (%) | Tensile Strength (N/mm²) | Tear Strength (N/mm) | Elongation at Break (%) | Tensile Strength (N/mm²) | Izod Impact Strength (kJ/mol) |
|---|---|---|---|---|---|---|---|---|
| 0 | 18.3 (3) | 9.80 (1.62) | 322 (33.6) | 3.75 (1.06) | 9.46 (0.58) | 49 (3.52) | 1.25 (0.1) | 330 (14.4) |
| 5 | 9.5 (2.5) | 20.21 (1.64) | 185 (13.6) | 9.61 (0.74) | 14.75 (0.51) | 31 (3.16) | 2.01 (0.12) | 810 (38.9) |
| 10 | 4.5 (0.5) | 22.40 (1.35) | 80 (3.28) | 12.37 (0.63) | 17.76 (0.32) | 21 (2) | 3.10 (0.34) | 1530 (26.0) |
| 15 | 4.0 (0.25) | 23.47 (1.26) | 132 (4.83) | 13.37 (1.16) | — | 24 (1.4) | 3.14 (0.19) | 1180 (14.14) |

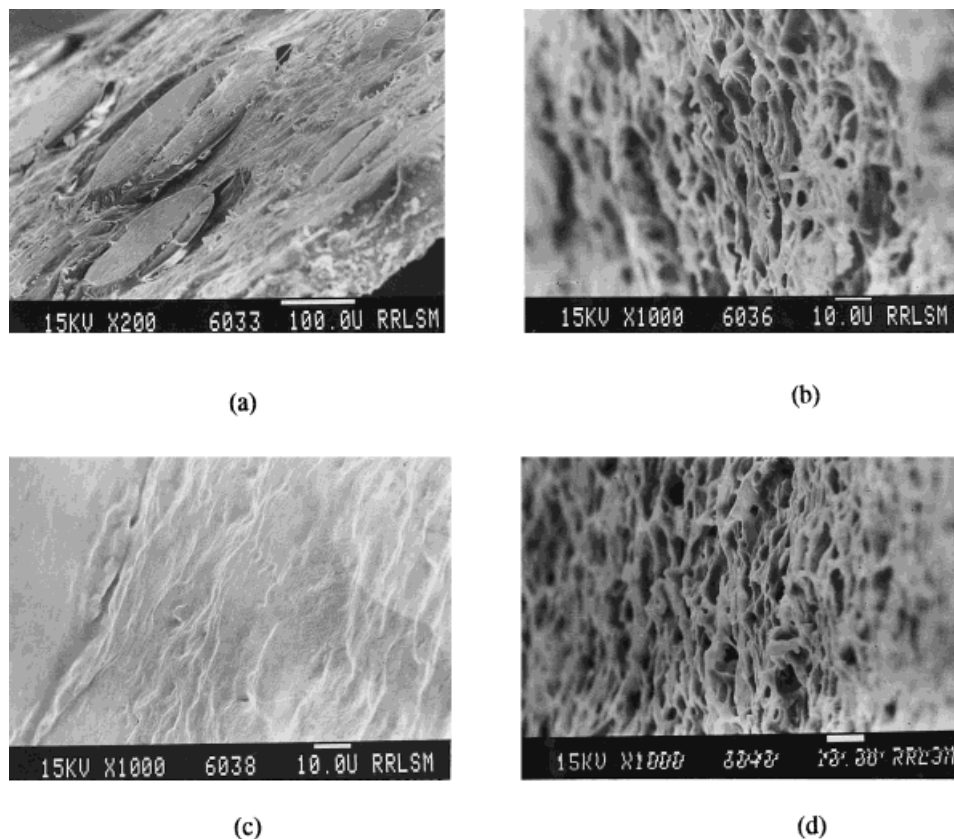Standard deviation values are given in parentheses.

**Figure 7** Tensile fractographs of 50/50 NR/PMMA blends: (a) 0%, (b) 5%, (c) 10%, and (d) 15% graft copolymer.

implies insufficient adhesion between the domains and the matrix. Consequently, the tear strength is also low as shown by the experiment. Addition of the graft copolymer changed the failure surface from a brittle to a ductile type as evidenced by the presence of fibrils and microbridges on the fracture surface [Fig. 8(b,c)]. Microbridges between the phases is an indication of strong interphase adhesion.

## CONCLUSION

The morphology and mechanical properties of NR/PMMA blends were studied as a function of blend ratio and compatibilizer concentration. The mechanical properties of the incompatible blends are found to be influenced by the blend ratio. Tensile strength, tear strength, and the Young's modulus decrease with increase in NR content. Various composite models were used to fit the experi-

mental data. Coran's equation is found to agree with the experimental value. Addition of a compatibilizer reduces the domain size followed by a leveling-off at higher graft copolymer concentration.

Tensile strength, tear strength, and Izod impact strength show considerable improvement by the addition of the graft copolymer. The properties attain an optimum value when the reduction in domain size is maximum. Interfacial adhesion between the two homopolymers increases by the addition of the graft copolymer and, consequently, the mechanical properties increase. Solution-cast blends exhibit better mechanical properties as compared to melt-mixed samples due to degradation at processing conditions. SEM studies of the failure surfaces indicate no adhesion between the components in the uncompatibilized system. The presence of microfibrils on the fracture surface of the compatibilized system indicates improved interface adhesion.
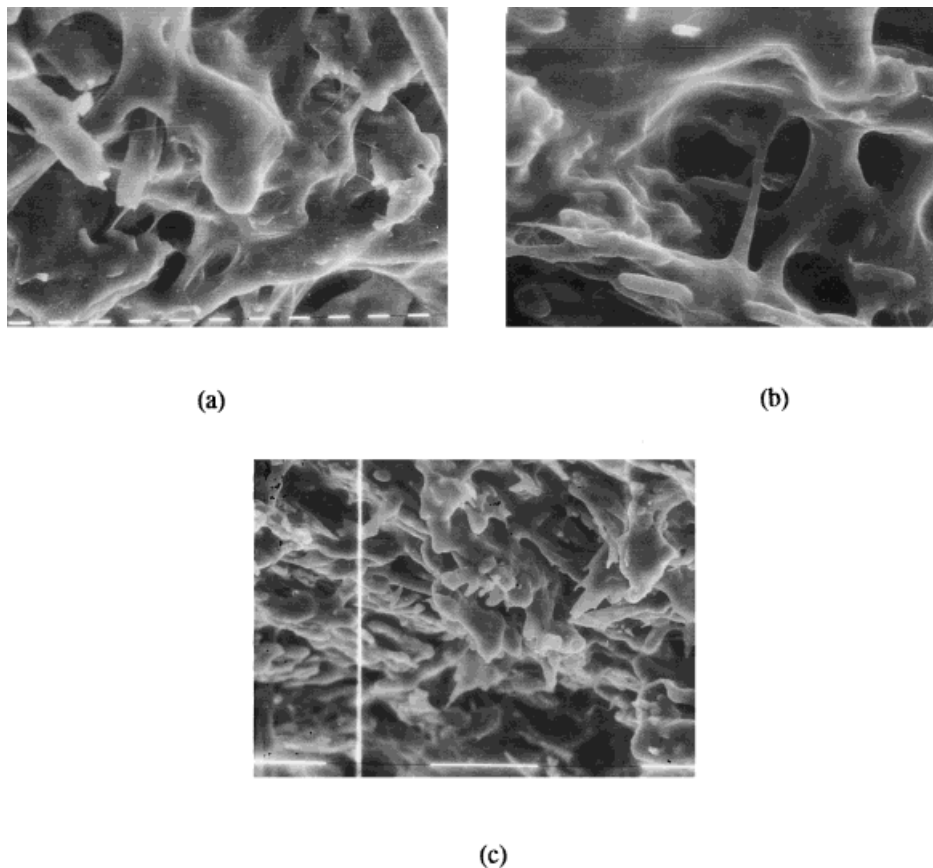
**Figure 8**   Tear fractographs of 50/50 NR/PMMA blends: (a) 0%, (b) 5%, and (c) 10% graft copolymer.

## REFERENCES

1. G. E. Molau, in *Block Polymers,* Plenum Press, New York, 1970, p. 79.
2. G. E. Molau and H. Keskkula, *Appl. Polym. Symp.,* **7,** 35 (1968).
3. D. R. Paul, in *Polymer Blends,* D. R. Paul and S. Newman, Eds., Academic Press, New York, 1978, Chap. 12.
4. D. R. Paul and S. Newman, in *Polymer Blends,* D. R. Paul and S. Newman, Eds., Academic Press, New York, 1978, Vol. 1.
5. B. M. Walker, Ed., *Handbook of Thermoplastic Elastomers,* Van Nonstrand Reinhold, New York, 1979.
6. A. D. Thorn, *Thermoplastic Elastomers: A Review of Current Information,* Rubber and Plastics Research Association of Great Britain, Shawbury, England, 1980.
7. J. C. West and S. L. Cooper, in *Science and Technology of Rubber,* F. R. Eirich, Ed., Academic Press, New York, 1978, Chap. 13.
8. L. Mullins, *Rubb. Devel.,* **31,** 92 (1978).
9. A. Y. Coran and R. Patel, *Rubb. Chem. Technol.,* **53,** 141 (1980).
10. A. Y. Coran and R. Patel, *Rubb. Chem. Technol.,* **54,** 91 (1981).
11. A. Y. Coran and R. Patel, *Rubb. Chem. Technol.,* **54,** 892 (1981).
12. W. K. Fisher, U.S. Pat. 3,758,643 (1971).
13. D. S. Campbell, D. J. Elliott, and M. A. Wheelans, *NR Technol.,* **9,** 21 (1978).
14. A. Y. Coran and R. Patel, *Rubb. Chem. Technol.,* **54,** 91 (1981).
15. A. Y. Coran and R. Patel, *Rubb. Chem. Technol.,* **54,** 892 (1981).
16. A. Y. Coran and R. Patel, *Rubb. Chem. Technol.,* **55,** 116 (1982).
17. S. Thomas, B. Kuriakose, B. R. Gupta, and S. K. De, *J. Mater. Sci.,* **21,** 711 (1986).

18. S. Thomas, *Mater. Lett.,* **5,** 360 (1987).
19. J. George, L. Prasanna Kumari, P. Kozhy, K. T. Varughese, and S. Thomas, *Polym. Plast. Technol. Eng.,* **34,** 581 (1995).
20. S. George, R. Joseph, K. T. Varughese, and S. Thomas, *Polymer,* **36,** 4405 (1995).
21. R. Asaletha, M. G. Kumaran, and S. Thomas, *Polym. Plast. Technol. Eng.,* **34,** 633 (1995).
22. S. Thomas, B. Kuriakose, B. R. Gupta, and S. K. De, *J. Mater. Sci.,* **21,** 711 (1986).
23. S. Thomas, B. R. Gupta, and S. K. De, *J. Mater. Sci.,* **22,** 3209 (1987).
24. K. C. Dao, *Polymer,* **25,** 1527 (1984).
25. Z. Oommen and S. Thomas, *Polym. Bull.,* **31,** 628 (1993).
26. Z. Oommen, M. R. G. Nair, and S. Thomas, *Polym. Eng. Sci.,* **36,** 151 (1996).
27. E. Martuscelli, F. Riva, C. Sellitti, and C. Silvestre, *Polymer,* **26,** 270 (1985).
28. Z. K. Walczuk, *J. Appl. Polym. Sci.,* **17,** 169 (1973).
29. D. Heikens and W. Barentsen, *Polymer,* **18,** 69 (1977).
30. N. E. Nielsen, *Rheol. Acta,* **13,** 86 (1974).
31. J. C. Halpin, *J. Compos. Mater.,* **3,** 732 (1970).
32. A. Y. Coran, in *Handbook of Elastomers—New Development and Technology,* A. K. Bhowmick and H. L. Stephens, Eds., Marcel Dekker, New York, 1988, p. 249.
33. W. M. Barentsen and D. Heikens, *Polymer,* **14,** 579 (1973).
34. S. Thomas and R. E. Prud'homme, *Polymer,* **33,** 4260 (1992).
35. R. J. M. Borggreve, R. J. Gaymans, and H. M. Eichenwald, *Polymer,* **30,** 78 (1989).
36. S. Wu, *Polymer,* **26,** 1855 (1985).
37. R. J. M. Borggreve, R. J. Gaymans, J. Schuijer, and J. F. Ingen Housz, *Polymer,* **28,** 1489 (1987).
38. S. Shaw and R. P. Singh, *J. Appl. Polym. Sci.,* **40,** 685 (1990).
39. R. N. Santra, B. T. Samantaray, A. K. Bhowmick, and G. B. Nando, *J. Appl. Polym. Sci.,* **49,** 1145 (1993).
40. W. M. Barentsen, D. Heikens, and P. Piet, *Polymer,* **19,** 119 (1974).